Exciton-polariton lasing and amplification based on exciton-exciton scattering in CdTe microcavity quantum wells

R. Huang,[1] Y. Yamamoto,[1,2] R. André,[3] J. Bleuse,[3] M. Muller,[3] and H. Ulmer-Tuffigo[3]
[1]*Quantum Entanglement Project, ICORP, JST, Edward L. Ginzton Laboratory, Stanford University, Stanford, California 94305*
[2]*NTT Basic Research Laboratories, Atsugishi, Kanagawa, Japan*
[3]*Dépt. de Recherche Fondamentale sur la Matière Condensée, CEA Centre d'Etudes de Grenoble, France*
(Received 18 June 2001; revised manuscript received 15 January 2002; published 5 April 2002)

We describe experiments demonstrating an exciton-polariton laser and amplifier based on an incoherent exciton-polariton reservoir in CdTe microcavity quantum wells. The gain mechanism is real excited exciton-exciton scattering, in which excitons created at large in-plane wave vectors are thermalized and accumulate at the bottleneck lower polariton states at smaller in-plane wave vectors. Because the exciton-exciton scattering rate for CdTe at the saturation density is higher than that for GaAs, the threshold for spontaneous polariton lasing is more easily reached in the case of CdTe with respect to GaAs. We demonstrate a high-gain amplification of bottleneck lower polaritons close to the lasing threshold. By performing a pulsed pump and probe experiment, we observe unambiguous evidence of real excited exciton-exciton scattering gain in the form of $\exp(\text{const}\, N_{\text{exc}}^2)$, where N_{exc} is the exciton-polariton reservoir population. This result is in sharp contrast to the recently demonstrated parametric polariton amplifier based on virtual coherent four wave mixing, in which gain is proportional to $\exp(\text{const}\, N_{\text{exc}})$. [P.G. Savvidis *et al.*, Phys. Rev. Lett. **84**, 1547 (2000)].

DOI: 10.1103/PhysRevB.65.165314 PACS number(s): 71.36.+c, 42.55.Sa

I. INTRODUCTION

The optical laser and the atom laser are examples of the profound analogies between electromagnetic waves and de Broglie (matter) waves. A composite massive bosonic particle, such as a neutral atom or an exciton, can be amplified by the so-called final state stimulation. It is well known that there are two types of amplifiers for electromagnetic waves: a negative-conductance amplifier and a nonlinear-susceptance amplifier. A negative-conductance amplifier is based on an incoherent gain element, for which a laser amplifier is a classic example. A nonlinear-susceptance amplifier is based on coherent wave mixing between a pump, a signal, and an idler, for which a parametric amplifier is a classic example. Recently, Bose-Einstein condensates of alkali atoms,[1,2] and coherent exciton-polaritons produced by a pump laser,[3] illuminated by a different frequency probe laser beam, were used to demonstrate the second-type amplifier, that is, phase-coherent parametric amplification of matter waves. Matter-wave amplification of the first type is yet to be demonstrated but very attractive. In particular for an excitonic system, electrically injected incoherent excitons[4] can construct an amplifier and laser without requiring a coherent pump laser. Earlier work on optically inactive excitons in CuO_2 utilized the relatively slow phonon scattering process so that the observed gain is very small.[5]

Microcavity exciton-polaritons[6] are the strongly coupled quasi-particles formed by a photon mode confined by a microcavity and an exciton mode enclosed by a quantum well. A proposed polariton laser, which converts a nonequilibrium reservoir of excitons into a ground state lower polariton (LP) by acoustic phonon scattering,[7,8] has the same and fundamental problem as in CuO_2 of a slow phonon emission rate compared to a relatively fast polariton decay rate.[9,10] The exciton-exciton scattering process, combined with the acoustic phonon scattering process, was recently proposed as a means of efficiently converting initially injected reservoir excitons, in a large in-plane wave vector ($k_{\|}$) region outside of the strong coupling regime, into bottleneck LPs with a smaller $k_{\|}$ (Ref. 11) [see Fig. 1(a)]. The formation of the polariton reservoir shown in Fig. 1(a) is due to a thermalization process which depends on acoustic phonon and exciton-exciton scattering from the initial resonantly injected polariton population. The bottleneck effect is due to the inhibited relaxation of polaritons from the reservoir to the strongly coupled region, because of the reduced density of states of the small in-plane momentum lower polaritons. Because of this reduced relaxation rate, and relatively long radiative lifetime, polaritons in the reservoir can accumulate to form a phase space density large enough to achieve polariton lasing. The final state stimulation effect in the exciton-exciton scattering process was observed with the presence of an externally injected ground state LP in GaAs microcavities,[12] but the observed gain was negligibly small, and exciton bleaching occurs before spontaneous polariton lasing happens. The rate of exciton-exciton scattering is material dependent, and for small momentum exchange, is dominated by the exchange interaction:[11]

$$R_{\text{exc-exc}} \propto |M|^2 n_{\text{exc}}^2 \propto E_B^2 a_B^4 n_{\text{exc}}^2, \tag{1}$$

where M is the matrix element of electron-electron and hole-hole exchange interactions, n_{exc} is the exciton density, E_B is the exciton binding energy, and a_B is the exciton Bohr radius. For typical parameters of quantum well excitons, the rate of exciton-exciton scattering evaluated at the exciton saturation density, defined by $n_{\text{exc}}^{\text{sat}} \approx 0.117/(\pi a_B^2)$, is 9 times larger in the CdTe system compared to that of GaAs.[13]

 ©2002 The American Physical Society

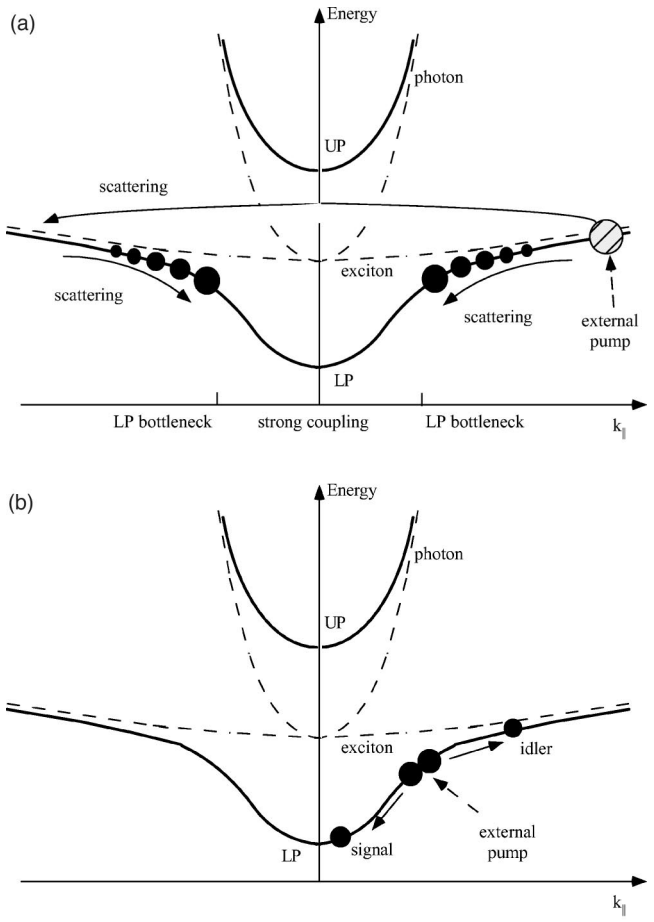

FIG. 1. (a) The operational principle of an exciton-polariton laser, in which optically excited excitons are transferred and piled up in the bottleneck regime by the exciton-exciton scattering process and the exciton-acoustic phonon scattering process. The area of the dark filled circles indicates the population at a particular $k_\parallel$. The bottleneck polaritons acquire a maximum population because of a reduced thermalization rate into lower energy polaritons due to the reduced density of states and a relatively long radiative lifetime due to reduced photon admixture. (b) The basic scheme of a parametric polariton amplifier based on the coherent four-wave mixing process between two pump, signal, and idler waves.

In contrast to the present polariton laser and amplifier based on the exciton-exciton scattering among incoherent bottleneck polariton populations, the recent experiments of parametric polariton amplifiers[3] utilize the coherent four-wave mixing process between two pump, signal, and idler waves, as shown in Fig. 1(b). Energy and momentum must be conserved between the initial and final states in the coherent process. The maximum incident angle θ_M of the pump beam, which satisfies the energy and momentum conservation laws, is for CdTe about $\theta_M \approx 13.5°$, and the signal state emission angle is in the range of 0 to 5°.[14] If the pump angle θ_p becomes larger than θ_M, which is the case in our experiment ($\theta_p \approx 25°$), such a coherent four-wave mixing process disappears and the injected excitons thermalize to the bottleneck polariton by elastic and inelastic scattering processes shown in Fig. 1(a).

In this paper we demonstrate spontaneous lasing and high-gain amplification of bottleneck polaritons, based on incoherent and quasiequilibrium polariton reservoirs in CdTe microcavities. By utilizing optical pump and probe laser beams, we show that the gain mechanism is not coherent four wave mixing, but rather, real excited exciton-exciton scattering.

II. LASING EXPERIMENTS

We used a microcavity sample grown by solid-source molecular beam epitaxy in the II-VI materials system. The entire microcavity structure is monolithic, including the distributed-Bragg reflector (DBR) mirrors, spacer layers, and quantum wells. The sample has two 80 Å CdTe quantum wells at the center, antinode position of the $\lambda/2$ $Cd_{0.6}Mg_{0.4}Te$ cavity region. The DBR mirrors are made of alternating index $\lambda/4$ layers of $Cd_{0.75}Mn_{0.25}Te$ and $Cd_{0.4}Mg_{0.6}Te$, with 16.5 (20) pairs on the top (bottom). The normal-mode splitting at zero detuning is 8.4 meV. During the experiments, the sample temperature is maintained at $T = 4.5$ K in a liquid helium cryostat.

Figure 2(a) shows the bottleneck polariton emission intensity, measured at the detection angle of 13° in air, versus the total exciton reservoir population, created by the pump laser pulse. The pump beam is from a mode-locked $Ti:Al_2O_3$ laser with a pulse duration of 1 ps and a repetition rate of 76 MHz. The maximum pump power is about 40 mW in this experiment. These results are similar to earlier nonlinear photoluminescence measurements on II-VI samples,[15,16] and on III-V samples.[17] The exciton at an in-plane wave vector of $k_\parallel = 3.5 \times 10^4$ cm^{-1} (incident angle $\theta_p = 25°$ in air), a region where the LP is nearly entirely excitonic in character, is excited by the pump laser. We monitor the bottleneck LP emission at approximately $k_\parallel = 1.8 \times 10^4$ cm^{-1} (emission angle of 13° in air). For a small initial exciton population, the observed emission is dominated by LP's created via acoustic phonon emission, leading to a linear dependence in the integrated LP emission as a function of initial exciton population. As the initial exciton population is increased above about 9×10^5 excitons/pulse,[18] a polariton laser threshold is observed. The corresponding exciton density is approximately 7×10^{10} cm^{-2},[18] which is nearly an order of magnitude smaller than the saturation density of 5×10^{11} cm^{-2} for CdTe QW excitons. The observed LP emission intensity corresponds to a LP population per transverse mode equal to ~ 1 at the threshold,[18] which suggests the nonlinear increase of the LP emission intensity is related to the onset of bosonic final state stimulation. To model the results shown in Fig. 3(a), we use the coupled discrete rate equations for the LP with different in-plane momenta,[11] with the CdTe parameters for the exciton-exciton and exciton-acoustic phonon scattering coefficients (solid line).

By using angular-resolved detection, we can map out the energy versus in-plane momentum for the LP, shown in Figs. 2(b) and 2(c). The detector is now swept over a range of emission angles to measure the polariton emission spectra as a function of angle. Below laser threshold, in Fig. 2(b), the bottleneck emission from the LP is seen at large in-plane wave vector, centered at about $k_\parallel = 3 \times 10^4$ cm^{-1} (emission

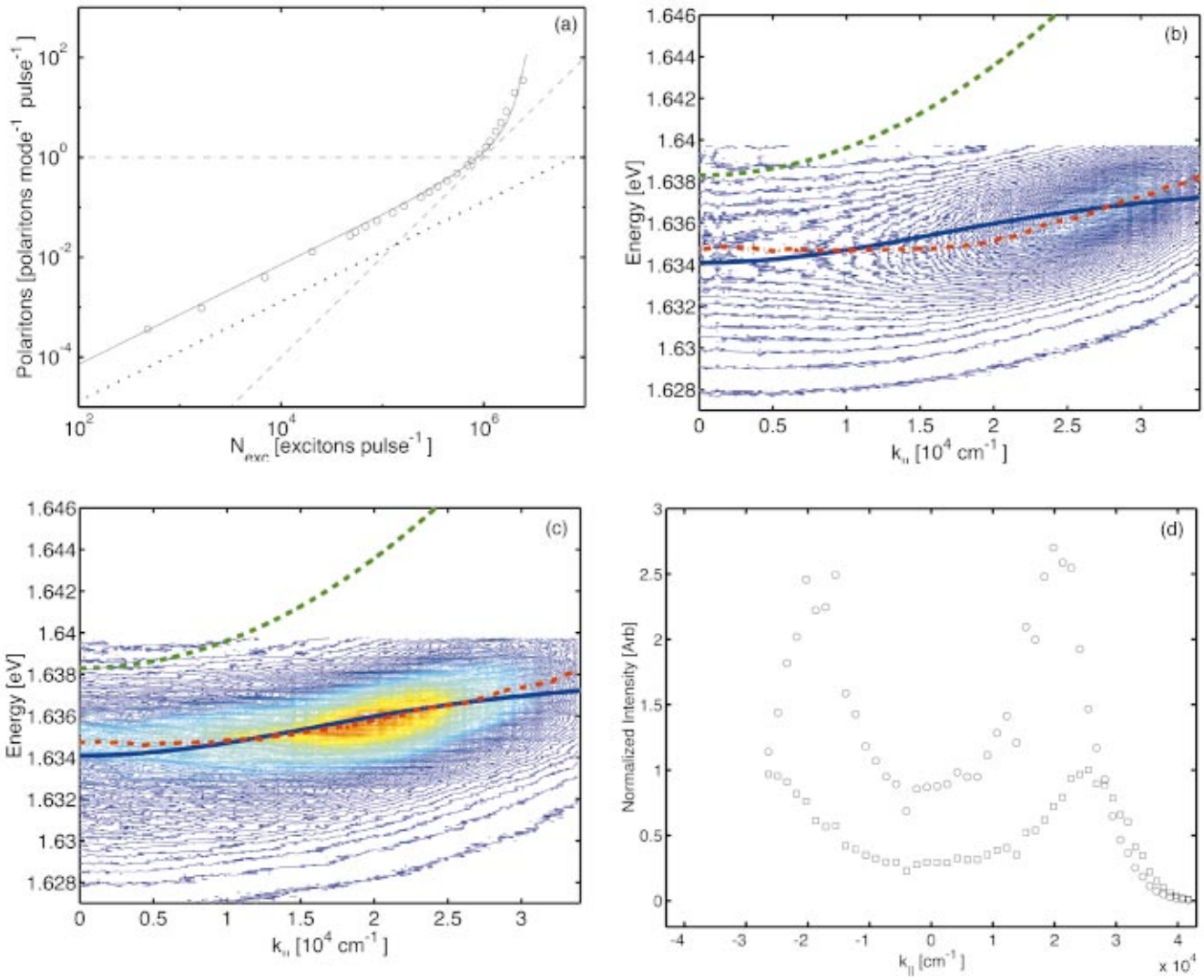

FIG. 2. (Color) (a) Integrated bottleneck LP emission intensity as a function of initial exciton population. The open circles indicate the experimental data, while the solid line indicates the theoretical prediction. Slope one is shown in the dotted line, slope two is indicated by the dashed line, while the dot-dashed line indicates a bottleneck polariton population of $N_{\mathrm{LP}}=1$. (b) The polariton spectra taken as a function of in-plane wave vector. The system is below laser threshold, and the solid line indicates the LP dispersion relation, the dashed line indicates the bare photon dispersion, and the dot-dashed line indicates the experimentally measured LP dispersion. (c) The polariton spectra taken as a function of in-plane wave vector. The system is above the laser threshold, and the solid line indicates the LP dispersion relation, the dashed line indicates the bare photon dispersion, and the dot-dashed line indicates the experimentally measured LP dispersion. (d) The LP emission intensity versus in-plane wave vector for the pump rates below (squares) and above (circles) laser threshold. LP emission intensities are normalized to the input pump power.

angle of 21° in air). Above the laser threshold, the LP population is peaked at about $k_{\parallel}=2\times10^{4}\ \mathrm{cm}^{-1}$ (emission angle of 14° in air). As the pump power is increased to past the laser threshold, the maximum of the LP emission continually shifts towards smaller $k_{\parallel}$, as shown in Fig. 2(c). This effect is predicted by the rate equation theory.[11] The theoretical dispersion curves for the cavity photon and LP are plotted in Figs. 2(b) and 2(c) (dashed and solid lines, respectively). Also plotted on these figures are the experimental LP dispersions (dot-dashed lines), obtained from the peak energies of the polariton distribution at each in-plane wave vector. The experimental and theoretical dispersions for the LP match to within approximately 1 meV over the entire range of in-plane wave vectors measured. It is clear from the effective mass of the lasing mode $m=\hbar^{2}k_{\parallel}(dE/dk_{\parallel})^{-1}\gg m_{\mathrm{ph}}$ (cavity photon effective mass), that the observed nonlinear emission is not a normal photon laser but a polariton laser. The LP emission intensity versus emission angle is plotted in Fig. 2(d) for the pump rates below and above threshold. Note that the bottleneck emission is symmetric, that is, $N_{LP,+k}\approx N_{LP,-k}$. This is a unique and unambiguous signature of the polariton laser based on incoherent exciton-polariton reservoirs [see Fig. 1(a)]. In the parametric polariton amplifier, the emission is strongly asymmetric [see Fig. 1(b)], that is, $N_{LP,+k}\gg N_{LP,-k}$.[19]

The dispersion of the polariton laser also shows that the lasing is not due to localized excitons. The reason for this is that the measured dispersion clearly features the effective

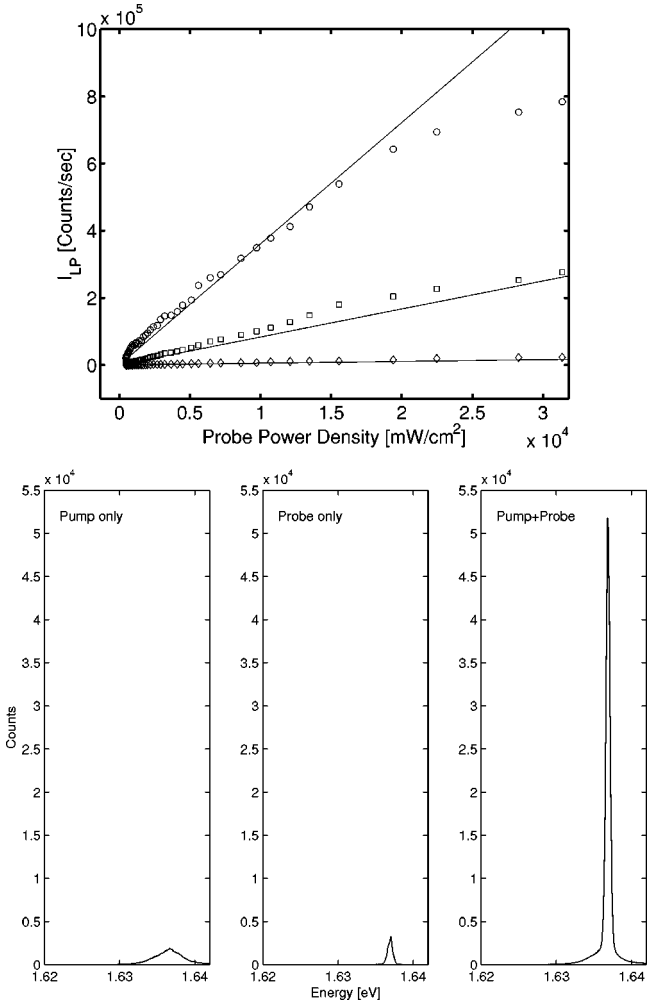

FIG. 3. The reflected probe intensity as a function of input probe power for three different total exciton populations: circles, $N_{\mathrm{exc}}=3.4\times10^6$ excitons/pulse, squares, $N_{\mathrm{exc}}=1.6\times10^6$ excitons/pulse, and diamonds, $N_{\mathrm{exc}}=4.1\times10^5$ excitons/pulse. The solid lines represent the numerical integration of the rate equation 2. Inset: Observed probe spectra for pump only, probe only, and simultaneous pump and probe excitation.

mass of the polariton. If the lasing were due to localized excitons, the dispersion would be constant in energy because the energy of a localized exciton on this scale is constant as a function of wave vector.

III. AMPLIFICATION EXPERIMENTS

In order to demonstrate the amplification process, we performed experiments probing the gain near the polariton laser threshold. We use a pump and probe set up, in which a pump pulse excites the large in-plane momentum excitons in a similar manner to the experiments described above. The pump and probe pulses are produced by the Ti:Al_2O_3 laser pulse (with a pulse width of 200 fs) by spectral filtering with two gratings, and are independently tunable in center frequency. The probe pulse is filtered such that it has a narrower bandwidth than the pump pulse. The pump bandwidth is about 3 meV, and selectively excites the excitons with $k_{\|}=3.5\times10^4$ cm^{-1} (incident angle $\theta_p=25°$ in air). The probe bandwidth is about 0.6 meV, and selectively excites the bottleneck LP near its lasing energy of $E=1.636$ eV, and at an in-plane wave vector of $k_{\|}=1.8\times10^4$ cm^{-1} (or $\theta=13°$). The probe beam then produces a narrow bandwidth bottleneck LP population, which is amplified by the surrounding LP populations. Both pump and probe beams are horizontally polarized, so that there is no selective exciton spin excitation. The detector is positioned to detect the reflected probe beam from the sample.

The detected spontaneous emission spectrum, induced by the pump beam, is shown in the leftmost inset of Fig. 3, labeled ''pump only.'' In the center inset, the detected probe signal is shown, corresponding to the situation where the pump beam is blocked. This spectrum is labelled ''probe only.'' When both pump and probe are incident on the sample, with zero time delay between the pump and the probe, a large amplification of the probe beam is observed. This amplified probe spectrum is shown in the right most inset of Fig. 3.

In Fig. 3, main figure, we plot the reflected probe emission intensity when the incident probe beam excites the bottleneck LP state. The three different initial exciton populations are chosen close to the polariton laser threshold. The pump and probe pulses have zero time delay between them for this measurement. We see that the reflected probe intensity is linear as a function of input probe intensity, and then saturates at larger probe powers. The linearity of the reflected probe intensity as a function of input probe intensity is a signature of final state stimulation. The dynamics of the bottleneck LP population is modeled by[11]

$$\frac{dN_{\mathrm{LP}}}{dt}=P_{\mathrm{LP}}-\frac{N_{\mathrm{LP}}}{\tau_{\mathrm{LP}}}+a_{\mathrm{LP}}N_{\mathrm{exc}}(1+N_{\mathrm{LP}})+b_{\mathrm{LP}}N_{\mathrm{exc}}^2(1+N_{\mathrm{LP}}), \tag{2}$$

where τ_{LP} is the LP lifetime, P_{LP} is the external injection rate of the LP, $a_{\mathrm{LP}}=47$ 1/s is the acoustic phonon scattering rate from the exciton-polariton reservoir, and $b_{\mathrm{LP}}=0.45$ 1/s is the exciton-exciton scattering rate from the exciton-polariton reservoir. We find that the gain is nearly independent of the LP injection rate P_{LP}. As P_{LP} is increased beyond a certain value, gain saturation occurs, and the system enters into the nonlinear regime. When the LP mode occupation number becomes comparable to the initial exciton population, the exciton states become depleted, reducing the stimulated scattering rate into the LP final state.

Next, to probe the physical origin of the gain, we show measurements of the gain dependence on the pump power. In Fig. 4(a), the gain as a function of pump power is plotted. The gain follows an exponential-type dependence which is well reproduced by the rate equation model (solid line). As shown in Figs. 4(b) and 4(c), the gain G is proportional to exp(const N_{exc}^2) in the high-gain regime, and $G-1$ is proportional to (const N_{exc}^2) in the low-gain regime. These experimental results directly indicate that the gain is provided by the real excited two-body exciton-exciton scattering process.

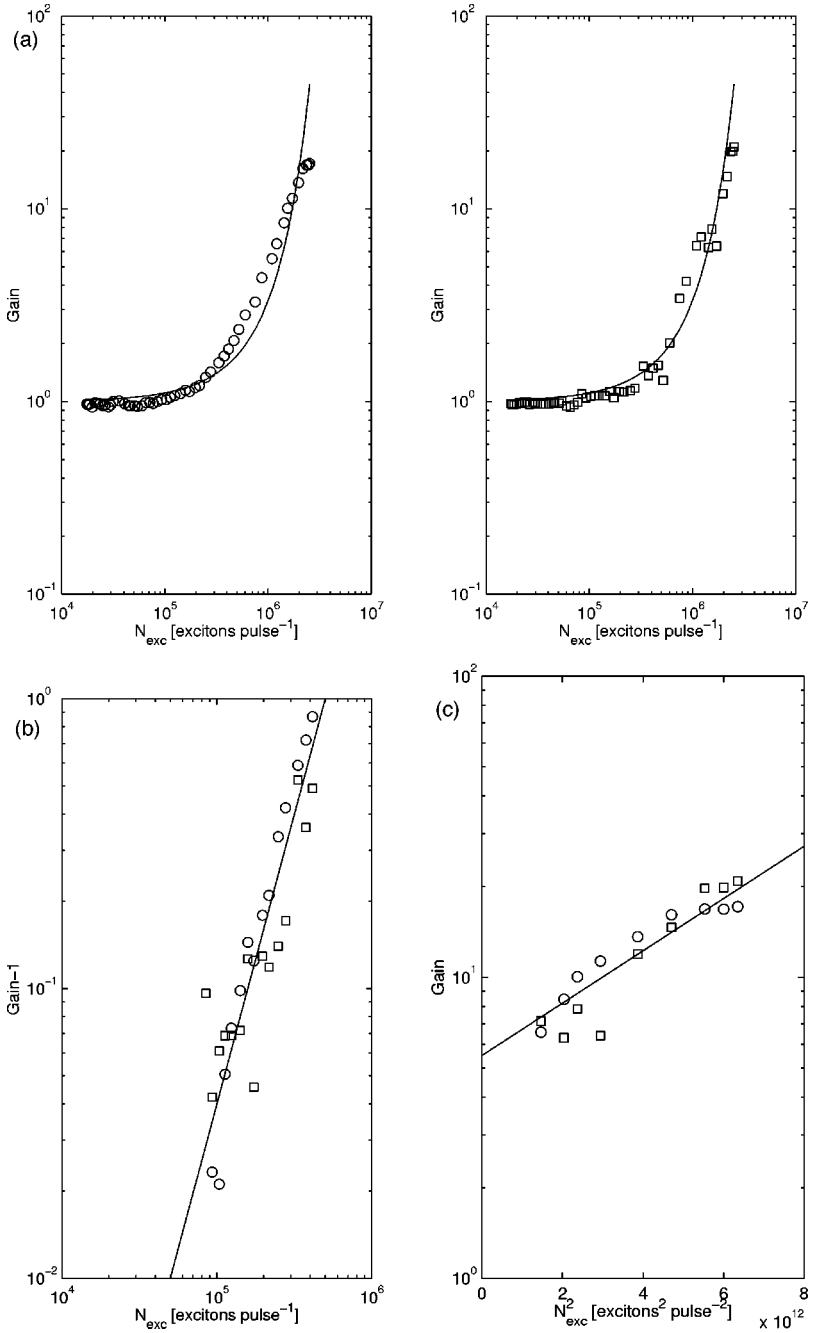

FIG. 4. (a) Gain as a function of pump power for two different probe power densities: circles, probe power density 2×10^4 mW/cm^2 and squares, 900 mW/cm^2. Solid line indicates rate equation solution. (b) Log-log plot for gain-1 as a function of initial exciton population, with same data as in (a). This plot is restricted to the low gain regime. Solid line has a slope of 2, which indicates that gain $g\approx1+\text{const}\ N_{\text{exc}}^2$ in the small gain region. (c) Semilog plot for gain as a function of the squared initial exciton population, restricted to the high gain regime. Solid line is linear, which indicates that $g\approx\exp(\text{const}\ N_{\text{exc}}^2)$ in the high gain regime.

The exp(const N_{exc}^2) dependence of the gain is conclusive evidence for the gain mechanism of real excited exciton-exciton scattering from incoherent and quasiequilibrium exciton-polariton distributions. This mechanism is distinctly different from the polariton parametric amplification process based on coherent four wave mixing.[3] In this case, the parametric gain is proportional to the pump intensity, that is, $g\propto\exp(\text{const}\ N_{\text{exc}})$.

The difference between coherent four wave mixing and real excitation exciton-exciton scattering is analogous to the difference between an optical parametric amplifier and a laser amplifier. This difference manifests in the exp(const $|E_p|$) gain dependence of the optical parametric amplifier, in contrast to the exp(const $|E_p|^2$) gain dependence of the laser amplifier, where $|E_p|$ is the pump laser amplitude. The physical reason for this distinction is that in the laser amplifier, real absorption of the pump photon occurs by a phase breaking transition. In the optical parametric amplifier, the pump photon is only virtually absorbed and split into signal and idler photons by the parametric amplifier medium. The parametric gain only exists for the time duration the pump and probe pulses overlap,[20,3] For the laser amplifier, the gain persists after the pump pulse has turned off, up to a time constant determined by the reservoir exciton-polariton lifetime. Parametric amplification can be considered to be frequency conversion of photons resonantly enhanced by polaritons, while laser amplification involves real absorption of photons followed by real scattering of

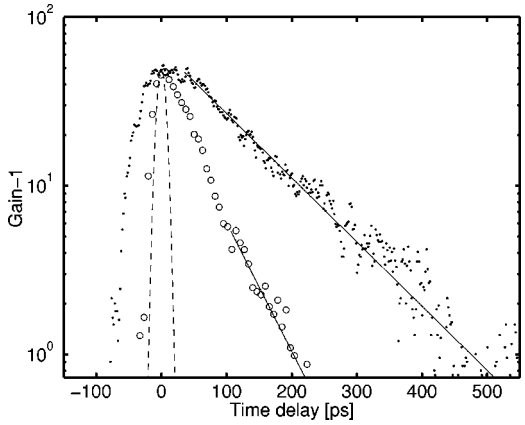

FIG. 5. Gain −1 as a function of time delay. Experimentally measured gain is in open circles. In the same plot, the intensity as a function of time for the bottleneck LP is shown in solid dots. Solid lines indicate exponential decay curves of 114 and 57 ps. The dashed line indicates the convolution of the pump and the probe pulse envelopes for comparison.

exciton-polaritons. The exp(const $|E_p|^2$) gain dependence also shows the difference between the polariton laser based on incoherent exciton-exciton scattering and a conventional photon laser, in which the gain dependence is exp(const $|E_p|$).

In Fig. 5, we plot the experimentally measured gain as a function of time delay between pump and probe. The time dependence of the gain clearly features an asymmetry about zero time delay, and is characterized by a relatively fast rise and then a relatively slow exponential decay. The exponential decay is due to the fact that the bottleneck polaritons have a characteristic decay time. The bottleneck polariton decay time has been measured separately by monitoring the emission directly using a streak camera. The solid dots in Fig. 5 represent the measured bottleneck polariton emission intensity as a function of time. The characteristic decay time is approximately 114 ps. The gain, however, has a characteristic decay time of approximately 57 ps in the small gain regime. The difference of a factor of 2 in the decay times is due to the N_{exc}^2 quadratic dependence of the gain mechanism.

We also note that the time dependence clearly indicates that the amplification is not provided by a coherent four wave mixing process. In coherent four wave mixing, the gain decays with a time constant that is given by the convolution of the pump and probe pulses, since the exciton dephasing time is comparable to or shorter than the pulse duration of a few picoseconds.[21] The convolution of the pump and probe pulses used in the present experiment amounts to 10 ps, which is much less than the exponential decay time of 57 ps observed in the experiment, as shown in the dashed line in Fig. 5.

IV. DISCUSSION

It is important to consider alternative possible origins of the gain in the polariton laser. We can rule out localized excitons, which have been observed in Ref. 22, as the possible origin of the polariton gain. In Fig. 2(c), we can estimate the ratio of the bottleneck polariton mass to the cavity photon mass $r = m_{\mathrm{LP},k=2\times10^4\ \mathrm{cm}^{-1}}/m_{\mathrm{ph},k=0} \approx 4.3$ (calculated from the experimental LP dispersion), as we would expect for a bottleneck polariton laser. In the case of $r=1$, we have a photon laser, and in the case of $r>10^3$, we have a direct exciton (free or localized) laser. In our case, $r\approx4.3$ indicates directly that this is a polariton laser, and not cavity filtered localized exciton emission, as reported in Ref. 22. In addition, our observation of stimulated polariton emission in the bottleneck region apparently differs from that in Ref. 23, in which final state stimulation is observed to arise at $k_{\|}=0$. A possible reason for this is that according to the rate equation analysis, for zero cavity detuning, the stimulated emission originates at the bottleneck region, and migrates towards $k_{\|}=0$ for larger pumping powers. In fact, we have observed this same trend in our experiments at larger pumps. It is possible that in Ref. 23, the normalized pump power per quantum well is higher than that used in our experiment.

The linear dependence of the reflected probe intensity on the incident probe intensity demonstrates that this phenomenon is due to the stimulated exciton-exciton scattering, where the final state LP population induced by the probe pulse stimulates more scattering into the final LP state. The dependence of the gain on the pump power demonstrates that the microscopic origin of the gain is the binary collision process of real excited exciton-exciton scattering. This dependence on pump power also rules out localized exciton involvement in the gain, as the exciton-exciton scattering involves only free excitons. The time delay dependence of the gain further confirms the mechanism of exciton-exciton scattering, in that the exponential decay time constant of the gain is one half the exponential decay time constant of the bottleneck polaritons. The time delay dependence also highlights the distinct difference between this gain mechanism and previously observed coherent four wave mixing,[3,21] because the decay time of the gain is much longer than the excitation pulse durations. Because of the large exciton-exciton scattering rate in CdTe, we are able to observe the high gain amplification of bottleneck polaritons.

We consider the possibility of a low threshold, electrically pumped polariton laser based on real excited exciton-exciton scattering. The proposed structure is a microcavity quantum well, in which a tunnel junction is fabricated so that bottleneck polaritons can be formed directly in the central quantum well by resonant tunnelling.[4] Using GaAs parameters for the polariton laser,[24] the threshold exciton density is $5\times10^9\ \mathrm{cm}^{-2}$, which corresponds to the threshold exciton population for a square 1 μm device of $N_{\mathrm{exc}}=50$. If the bottleneck polariton lifetime is 190 ps,[12] the threshold tunnel current is 42 nA. This threshold current is much smaller than that in a standard InGaAs/GaAs VCSEL, where threshold currents are about 50 μA for the same device dimension. A standard VCSEL requires the population inversion between the conduction and valence bands, while a bottleneck polariton laser does not need the population inversion. The polariton laser in GaAs and CdTe can only operate at low temperatures because the exciton binding energy is relatively small in these material systems. However, one can speculate

that improvements in the wide-band-gap materials, in which the exciton binding energy is relatively large so that the exciton is stable at room temperature, might allow for room temperature operation of a bottleneck polariton laser.

[1] S. Inouye, T. Pfau, S. Gupta, A.P. Chikkatur, A. Görlitz, D.E. Pritchard, and W. Ketterle, Nature (London) **402**, 641 (1999).

[2] M. Kozuma, Yoichi Suzuki, Yoshio Torii, Toshiaki Sugiura, Takahiro Kuga, E.W. Hagley, and L. Deng, Science **286**, 2309 (1999).

[3] P.G. Savvidis, J.J. Baumberg, R.M. Stevenson, M.S. Skolnick, D.M. Whittaker, and J.S. Roberts, Phys. Rev. Lett. **84**, 1547 (2000); R.M. Stevenson, V.N. Astratov, M.S. Skolnick, D.M. Whittaker, M. Emam-Ismail, A.I. Tartakovskii, P.G. Savvidis, J.J. Baumberg, and J.S. Roberts, *ibid.* **85**, 3680 (2000); J.J. Baumberg, P.G. Savvidis, R.M. Stevenson, A.I. Tartakovskii, M.S. Skolnick, D.M. Whittaker, and J.S. Roberts, Phys. Rev. B **62**, R16 247 (2000).

[4] H. Cao, G. Klimovitch, G. Björk, and Y. Yamamoto, Phys. Rev. Lett. **75**, 1146 (1995); G. Klimovitch, F. Tassone, Y. Yamamoto, and H. Cao, Phys. Lett. A **267**, 281 (2000).

[5] A. Mysyrowicz, E. Benson, and E. Fortin, Phys. Rev. Lett. **77**, 896 (1996).

[6] C. Weisbuch, M. Nishioka, A. Ishikawa, and Y. Arakawa, Phys. Rev. Lett. **69**, 3314 (1992).

[7] A. Imamoğlu and R.J. Ram, Phys. Lett. A **214**, 193 (1996).

[8] A. Imamoğlu, R.J. Ram, S. Pau, and Y. Yamamoto, Phys. Rev. A **53**, 4250 (1996).

[9] H. Cao, S. Pau, J.M. Jacobson, G. Bjork, Y. Yamamoto, and A. Imamoğlu, Phys. Rev. A **55**, 4632 (1997).

[10] M. Kira, F. Jahnke, S.W. Koch, J.D. Berger, D.V. Wick, T.R. Nelson, Jr., G. Khitrova, and H.M. Gibbs, Phys. Rev. Lett. **79**, 5170 (1997).

[11] F. Tassone and Y. Yamamoto, Phys. Rev. B **59**, 10 830 (1999).

[12] R. Huang, F. Tassone, and Y. Yamamoto, Microelectron. Eng. **47**, 325 (1999); R. Huang, F. Tassone, and Y. Yamamoto, Phys. Rev. B **61**, R7854 (2000).

[13] R. Huang, Ph. D thesis, Stanford University, 2000.

[14] C. Ciuti, P. Schwendimann, B. Deveaud, and A. Quattropani, Phys. Rev. B **62**, R4825 (2000).

[15] L.S. Dang, D. Heger, R. André, F. Boeuf, and R. Romestain, Phys. Rev. Lett. **81**, 3920 (1998).

[16] P. Kelkar, V. Kozlov, A. Nurmikko, C. Chu, J. Han, and R. Gunshor, Phys. Rev. B **56**, 7564 (1997).

[17] P. Senellart and J. Bloch, Phys. Rev. Lett. **82**, 1233 (1999).

[18] The initial exciton population per QW is estimated from the number of photons per pulse, multiplied by the estimated absorption in a CdTe quantum well, and multiplied by the measured coupling of photons into the microcavity. At threshold the pump power is about 9 mW, corresponding to 4.5×10^8 photons/pulse. The absorption in each QW is about 1%, and the fraction of photons coupled into the cavity is about 20%, so that threshold corresponds to 9×10^5 excitons/pulse. The excitation spot radius on the sample is about 20 μm, so that at laser threshold the exciton density is about $7\times10^{10}\mathrm{cm}^{-2}$. To estimate the detected LP mode density, the number of detected LP's is divided by the number of momentum states subtended by the detector, that is, $N_L=4\pi c^2 P_L/[\eta\omega_{\mathrm{cav}}^2(\sin\theta_1-\sin\theta_2)^2]$, where P_L is the number density of detected counts, η is the detector system quantum efficiency, θ_1 and θ_2 are the angles subtended by the detector, ω_{cav} is the cavity frequency, and c is the speed of light. At laser threshold, we measured $P_L\approx3\times10^7$ photons cm^{-2} sec^{-1}. For $\eta=0.005$, $\theta_1=12.52°$, and $\theta_2=12.50°$, we have $N_L\approx1$ polariton/mode.

[19] P.G. Savvidis, J.J. Baumberg, R.M. Stevenson, M.S. Skolnick, D.M. Whittaker, and J.S. Roberts, Phys. Rev. B **62**, R13278 (2000).

[20] M. Kuwata-Gonokami, S. Inouye, H. Suzuura, M. Shirane, R. Shimano, T. Someya, and H. Sakaki, Phys. Rev. Lett. **79**, 1341 (1997).

[21] G. Dasbach, T. Baars, M. Bayer, A. Larionov, and A. Forchel, Phys. Rev. B **62**, 13 076 (2000).

[22] A. Fainstein, B. Jusserand, and R. André, Phys. Rev. B **57**, R9439 (1998).

[23] F. Boeuf, R. André, R. Romestain, Le Si Dang, E. Pérrone, J.F. Lampin, D. Hulin, and A. Alexandrou, Phys. Rev. B **62**, R2279 (2000).

[24] F. Tassone and Y. Yamamoto, Phys. Rev. A **62**, 063809 (2000).